THE ASTROPHYSICAL JOURNAL, 194:77–85, 1974 November 15

ROCKET-ULTRAVIOLET SPECTRA OF KAPPA, LAMBDA, TAU, AND UPSILON SCORPII

EDWARD B. JENKINS, DONALD C. MORTON*, AND DONALD G. YORK
Princeton University Observatory
Received 1974 April 15; revised 1974 June 24

ABSTRACT

Rocket-ultraviolet spectra of τ Sco (B0 V), λ Sco (B1.5 V), κ Sco (B1.5 III), and υ Sco (B2 IV) are presented, covering ranges between 1160 and 1880 Å with resolutions of 0.8 and 2.2 Å. The close sequence of spectral and luminosity types permits a detailed comparison of how various spectral lines change with temperature and gravity. The advantages of specific features for a future ultraviolet classification system are discussed. In the main-sequence star τ Sco, the Si IV resonance lines show asymmetries that can be interpreted as outward mass motion with a velocity of up to 400 km s^{-1}.

Subject headings: early-type stars — line identifications — spectra, ultraviolet

I. NATURE OF THE OBSERVATIONS

As a continuation of the Princeton program for observing ultraviolet stellar spectra, an Aerobee rocket (KP 3.27) was launched from the White Sands Missile Range on 1971 May 28 at 9^h40^m UT by the Kitt Peak National Observatory. Spectra of κ, λ, τ, and υ Scorpii were obtained covering the wavelength ranges listed in table 1. A previous paper by Jenkins (1973) has reported the measurement of several interstellar absorption lines in these stars, while the present paper will discuss their atmospheric spectra. These observations provide an interesting comparison of early B spectral types. Some of these stars have been observed with the *Copernicus* satellite at higher resolution, but the data are not yet fully reduced. The rocket spectra will continue to be useful as a check on the background corrections for the *Copernicus* data and for studying features between 1450 and 1850 Å where the spectrometer signal-to-noise ratio is poor.

II. RECORDING AND REDUCTION OF THE DATA

The payload configuration was identical to that flown on two previous flights, as described by Morton *et al.* (1972*b*) and Morton, Jenkins, and Macy (1972*a*). The spectra were recorded on Kodak type 101-01 film which was developed in D19 developer for 4 minutes at 20° C. All of the stars are rather bright in the ultraviolet, and thus good exposure densities were obtained with spectra as much as 0.25 mm wide. The resulting signal-to-noise ratio of about 30:1, which was evaluated from the agreement of intensities recorded across the width of the spectra, surpasses the quality of the previous Princeton rocket spectra. The cameras yielded two sets of spectra, one at 0.8 Å and the other at 2.2 Å resolution (instrumental profile FWHM), which are shown in figure 1 (plate 1). These resolutions were obtained by limiting the rocket pointing jitter along the dispersion to only 1′ peak to peak by an attitude control system using a rate-integrating gyro. The spectrum lines are slanted because of a drift motion of the rocket parallel to the dispersion, which occurred along with an intentional drift in the perpendicular direction to widen the spectra.

As the rocket coasted from an altitude of 129.3 km through apogee at 178.7 km and then down to 172.9 km, high- and low-resolution spectra of κ, λ, and υ Sco were recorded over an exposure interval of 138.5 s. From 167.0 km down to 83 km the spectrum of τ Sco was obtained over a period of 91.2 s. A broad peak of continuous absorption by atmospheric oxygen centered on 1400 Å and narrow features at 1242 and 1206 Å became progressively stronger in the spectrum of τ Sco as the rocket descended, accounting for the spectrum's uneven appearance in figure 1.

The data were digitized by the microdensitometer at

* Guest Investigator, Kitt Peak National Observatory, which is operated by the Association of Universities for Research in Astronomy, Inc., under contract with the National Science Foundation.

TABLE 1

STARS AND WAVELENGTH COVERAGES

Star	MK*	V*	$B-V$*	E_{B-V}†	$v \sin i$‡ (km s^{-1})	Low Resolution (Å)	High Resolution (Å)
τ Sco....	B0 V	2.84	−0.24	0.06	20	1100–1810	1269–1517
λ Sco....	B1.5 IV	1.63	−0.22	0.03	237	1100–1810	1202–1509
κ Sco....	B1.5 III	2.42	−0.22	0.03	124	1110–1880	1326–1550
υ Sco....	B2 IV	2.70	−0.22	0.02	104	1100–1860	1212–1526

* Lesh (1972). † Johnson (1963). ‡ Uesugi and Fukuda (1970).

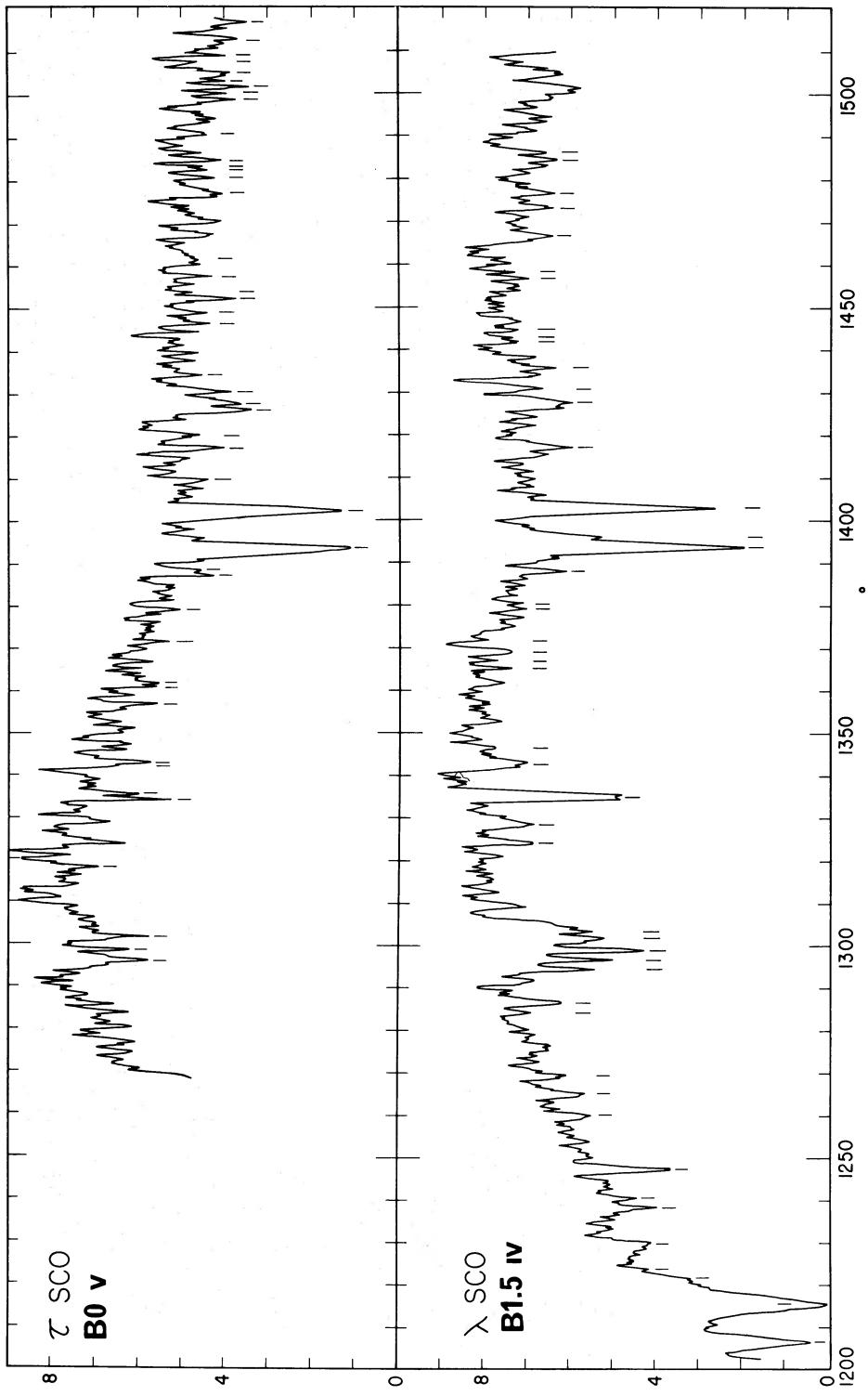

FIG. 2.—Intensity traces of the high-resolution spectra of τ Sco (B0 V) and λ Sco (B1.5 IV). No attempt has been made to correct the variations in the wavelength sensitivity of the spectrograph. The short vertical bars indicate the absorption features which are visible on the original photographs as well as on the densitometer trace.

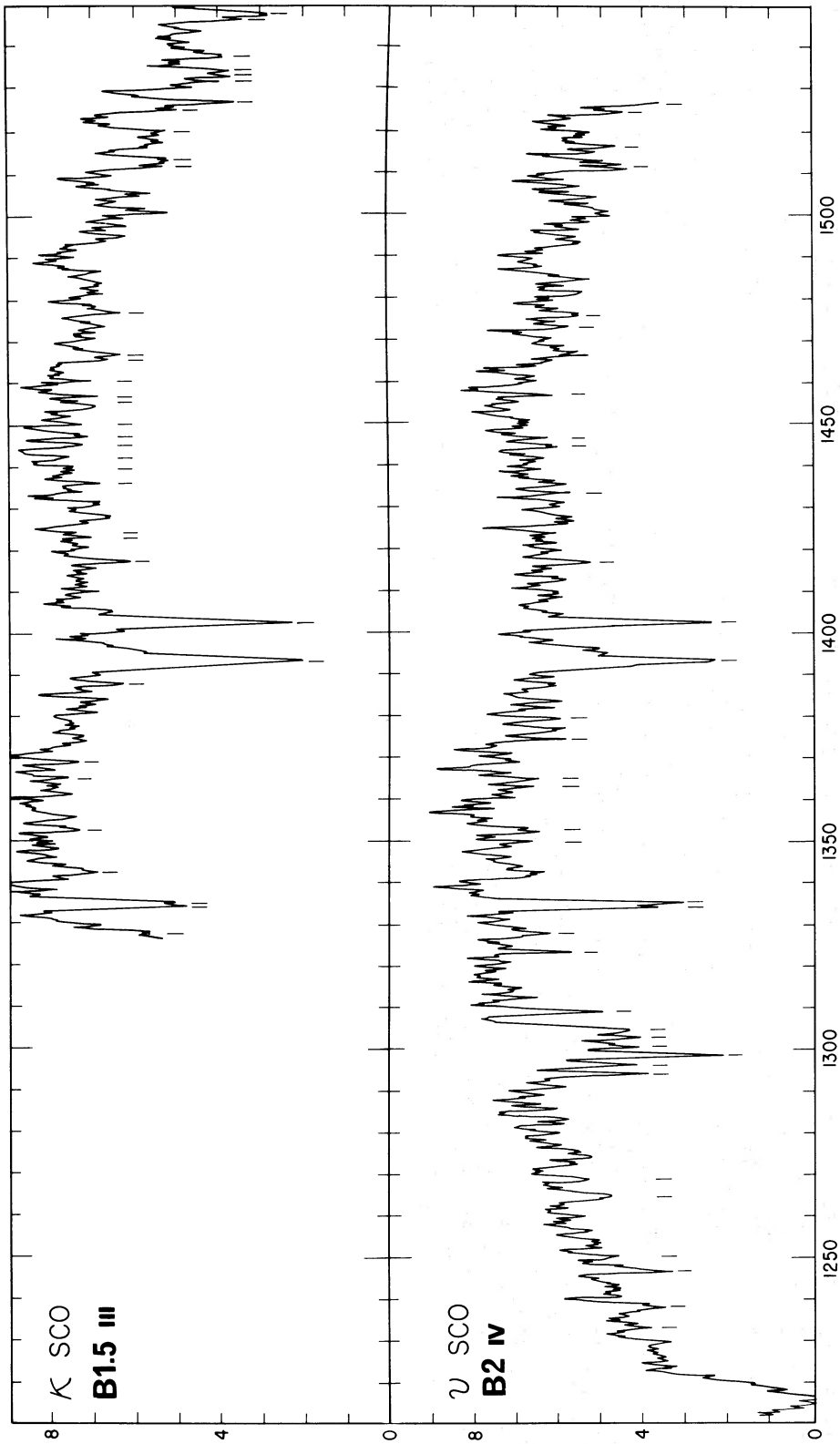

FIG. 3.—Intensity traces of the high-resolution spectra of κ Sco (B1.5 III) and υ Sco (B2 IV)

TABLE 2

OBSERVED WAVELENGTHS AND IDENTIFICATIONS

BOV τ Sco	B1.5 IV λ Sco	B1.5 III κ Sco	B2 IV υ Sco	Identifications
1175.2 b	1175.3 b	1175.4 b	1175.6 b	C III 4
1193.7 :b	1192 b	1192.7 b	1193.2 :b	Si II 5, S III 1
1200.0 :b	1200 b	1199.5 :b	1200.3 :b	N I 1
	High Disp.			
1205.8	1206.52 b	1205.9	1206.5	Si III 2, 11, 22
			High Disp.	
1215.7 b	1215.8 b	1215.8 b	1215.9 b	H I 1
	1221.7 b		1221.95:	
		1228.7		
	1229.9 b		1230.10:	C IV 11.14
	1233.62:		1233.55	
1238.2	1238.37		1238.58	N V 1
	1240.7			
1243.3		1242.0		N V 1
		1246.0		
1247.5	1247.33		1247.12	C III 9
	1250.06:b		1250.25	Si II 13.05
	1250.8 :b		1250.70	S II 1
1254.0	1253.8 :b		1253.9 :b	S II 1
		1258.5		
1260.5	1260.07 b		1260.45:	Si II 4
High Disp.	1264.8		1264.95	Si II 4
	1269.0		1269.20 b	
		1279.0		
		1282.9		
1284.03:	1284.23			N IV 18.87
	1286.55 b			
		1291.2		
1294.5 :	1294.52		1294.59	Si III 4
1295.30:b				
1296.52	1296.73		1296.58	Si III 4
1297.5 :b				
1298.92	1298.97		1298.94	Si III 4
		1300 :b		
1301.25	1301.0		1301.03	Si III 4
1302.06	1301.85			O I 2
	1303.43		1303.3	Si III 4
	1305.2 :		1305.1 :b	
1309.05:	1309.4 :		1304.35	Mg II
1318.35				
1324.1 :	1324.07		1323.78	C II 11
		High Disp.		
	1328.52 b	1328.2 b	1328.3	C I 4, Si III 48
		1329.79	1329.55	C I 4
1334.50	1334.55	1334.40	1334.60	C II 1
1335.77	1335.45	1335.77	1335.65	C II 1
	1342.0		1341.95:b	
1342.27		1342.43	1342.45:	Si III 39
	1343.05		1343.05:b	O IV
1343.32 b		1343.40		N II, O IV, Si III 39

BOV τ Sco	B1.5 IV λ Sco	B1.5 III κ Sco	B2 IV υ Sco	Identifications
1344.61:		1344.65:b		
1346.44	1346.55			N II, N III
			1349.35	
			1350.35	Al II
1352.8 :b	1352.8 :	1352.73 b	1352.70	Al III
			1353.55	
1357.1				
1361.25		1360.25 b		Si III 46, 68
1362.00	1362.00:b			Si III 38, 68
			1363.4	Si III 38
	1365.18	1365.10 b	1365.25	Si III 38
1367.1 :	1367.05	1367.28:		Si III 46
	1369.23	1368.9 b	1369.4 :b	Si III 46
1371.6 :	1371.8	1371.53:		
	1374.4		1374.90	
1376.26				
1379.35	1379.15			
			1379.72	Al III
	1380.45			
		1384.0 :	1384.0 :b	Al III
1387.52	1387.90	1387.79 b	1387.95:b	Si III 37
1394.00 b	1393.75 b	1393.60 b	1393.6 b	Si IV 1
	1396.0	1395.5 :	1395.65	
			1396.72	
1402.82 b	1402.90 b	1402.63 b	1402.80 b	Si IV 1
1410.00		1409.86		
	1417.3	1417.2	1417.3 b	Si III 9
1417.60				
1420.55		1420.50:b		
		1423.05		
1424.20:		1424.1	1424.23:	C III 19
1426.55 b		1426.35:b		C III 11.52
	1427.4 b		1427.3	
1428.0 b		1427.85:b		C III 11.52
1430.73	1430.9	1430.8 :	1431.0 :b	Si IV
	1433.8 :		1433.92 b	
1438.85 b				
	1435.82	1435.93	1436.0 :	Si III 61
1439.90:		1439.65		
1441.60:	1441.9	1441.95 b	1442.38:	Si III 3.05
	1442.9			
1444.62:	1444.65	1444.95 b	1444.02	
1446.65	1446.7 :b	1447.25 b	1446.96	Si III 3.05
1449.27				
	1450.25:	1450.07 b		
1452.72		1452.6 :		
1454.05				
		1455.50		
	1456.85	1456.7		
			1457.32	Si III 60

TABLE 2 (continued)

BOV τ Sco	B1.5 IV λ Sco	B1.5 III κ Sco	B2 IV υ Sco	Identifications
1457.90				
	1458.20			
1460.7 :b	1460.60:	1460.42:	1460.7 :b	
1461.9 :b	1461.57:		1461.78:	
1465.76:	1465.75:	1465.6	1465.40:b	
	1467.0 b	1466.7 b	1466.75:b	
1467.5 b		1467.58:		
1470.7 :b		1471.02:		
	1473.33	1473.43:b		
	1473.82		1473.60	
1476.80	1476.95	1476.69 b	1476.45 b	
1477.42 b				C III 12.04
1481.0		1481.25:		Mg II
1482.92				Mg II
1483.56				
	1484.65 b		1484.73:b	
1485.1 b				
1486.71:	1486.50 b	1486.45 b		
1491.35	1491.4 :b			
	1493.87:	1493.7 :	1493.80:b	
1495.1 :b	1494.90:b	1494.9 :b	1495.18:b	
1499.35	1499.40:b	1499.25:		
1500.70	1500.72:b	1500.52:	1500.35:b	Si III 36
	1501.67:b	1501.57:	1501.36:b	Si III 36, P III 6
1502.38 b				P III 6
1503.73				
1504.88	1504.8 :b	1504.5 :	1504.82:	P III 6
1505.6		1505.2 :		
1508.0				
1509.57	High Disp.	1509.33:		
1511.6		1511.5 :	1511.35:	
		1512.85 b	1512.58:	
1513.6 b	1513.0 :	1513.50	1513.40	Si III 94
			1516.82	
1517.3	1517.6 :b	1517.3 :b		
High Disp.		1519.95	1519.8 :b	
			1524.7	
		1525.28	1525.1	
1526.2				
		1527.00	1527.0	Si II 2
			High Disp.	
		1530.58		
		1531.9		C III 11.65, Fe III 84
1533.0	1532.5	1533.3	1532.4	Si II 2, Si IV 24
		1534.4		
		1538.1 b		Fe III 84
	1542.8			
		1546.87		
1548.2	1547.2	1548.20 b	1547.3	C IV 1
		High Disp.		
	1551.0	1550.3	1551.3	C IV 1, Fe III 84
		1571.5 :	1571.2	
			1575.5	
			1581.5	
1585.0 :		1584.3 :	1584. :	
		1594.2	1594 :b	
1601.3 :		1601.2	1601.6 :	Fe III 118
1607.5 :		1606.5 :	1606.5 :	Al III, Fe III 118
1610.8 :b	1611.5 :	1611.5	1611.5	Al III, Fe III 118
1621.3 :	1620.6 :	1621.0	1621.7	
		1622		
		1628.9	1628.7	N II
1630.5 :		1632.5	1632.5	
1640.5	1640.4 :	1640.4	1640.5	He II 12
1657.7 :	1658.2 :	1657.2 :	1657.3 :	C I 2
1662.3	1662.5	1662.5		
1671.0 b	1670.3 :	1671.0		Al II 2
	1672.7 :	1673.0	1673.3 :	Si III 58, Si IV 27
		1676.1		N II
			1677.3 :	
1678.5				
1682.7			1682.7 :	Ne II 7
1688.0	1687.5 :			N IV 20, Ne II 7
1718.3	1717.5			N IV 7
	1721.4	1722.0 :		C II 14.02, Al II 6
1723.5 b			1723 b	Al II 6
	1725.0			Al II 6
1748.0	1748.0	1748.0 :		N III 19
1752.0		1751.7 :		N III 19
1760.4	1760.7 :		1760.7	C II 10
		1765.2 :	1764.6	N II
	1775.0 :b	1776.2 :	1775.6	
		1790.3		
			1791.5 :b	
	1792.5 :			
	1798.2 :		1798.5	
			1802.0	Si III 51
		1807.5	1807.6 :	Si II 1
		1812.5 :	1813.0	
		1816.5 :	1816.3	Si II 1
		1830.5	1831.2	
		1834.9		
		1838.8		
		1845.4	1845.6 :	
		1855.0	1855.0	Al III 1
		1863.5		Al III 1
		1866.6		
		1872.0		

*Wavelengths in Å. A b notes a broad feature and a colon indicates the line was present on the intensity trace, but was not clearly visible on the photograph.

the Sacramento Peak Observatory which scanned the spectra and surrounding areas in a raster pattern with a slit 10 μ wide and 20 μ high. Figure 1 is actually a photographic replay of the densitometry, rather than a direct copy of the original flight film. The representations of the spectra in figure 1 were used to visually check the existence of spectral features and to identify possible film flaws or errors in densitometry. The final spectral tracings were synthesized by adding the individual intensities recorded along inclined lines parallel to the obvious spectral features. The derivations of intensities were based on H and D characteristic curves evaluated from laboratory exposures of the flight film. The method used relied on the absence of reciprocity failure for this type of film; Jenkins (1973) has summarized some reasons why this assumption is probably valid. Below the 1100 Å sensitivity limit of the low-resolution recordings some residual intensity was recorded. This light came from grating scatter, and the observed level was subtracted from the apparent intensities recorded for the stars at longer wavelengths. This low-level background has the virtue of fogging the film above the limiting exposure threshold.

The wavelength scales for the spectra are dependent upon both the camera configurations and the actual pointing of the rocket during the exposures. A method identical to that described by Morton *et al.* (1972*b*) was employed for evaluating the appropriate constants in the grating equations which related position on the film to wavelength in each spectrum. The wavelength scales incorporated a small linear shift in λ which gave the most satisfactory fit with easily identifiable features. Hence all wavelengths for a particular spectrum may be in error by a small constant, but our representation for the nonlinear scaling of λ against position should be reasonably accurate.

III. LINE IDENTIFICATIONS

Intensity tracings of the high-resolution spectra are shown in figures 2 and 3. In these and succeeding figures, the measured intensities have been multiplied by a scale factor to make the apparent height of the continua for the different stars nearly the same. Short vertical lines below many of the absorption features indicate where convincing lines appear across the full width of the spectra pictured in figure 1. In the photograph the distinguishability of various lines is somewhat dependent on their sharpness, which probably explains why small, narrow features show up better than larger, broad ones. The most prominent lines in these spectra are Si III λ1206.5, H I λ1215.7, C III λ1247.4, Si III $\lambda\lambda$1294.5–1303.2, C II $\lambda\lambda$1334.5, 1335.7, and Si IV $\lambda\lambda$ 1393.8, 1402.8.

Shortward of about 1450 Å, the *Copernicus* satellite (Rogerson, Spitzer *et al.* 1973) is providing detailed

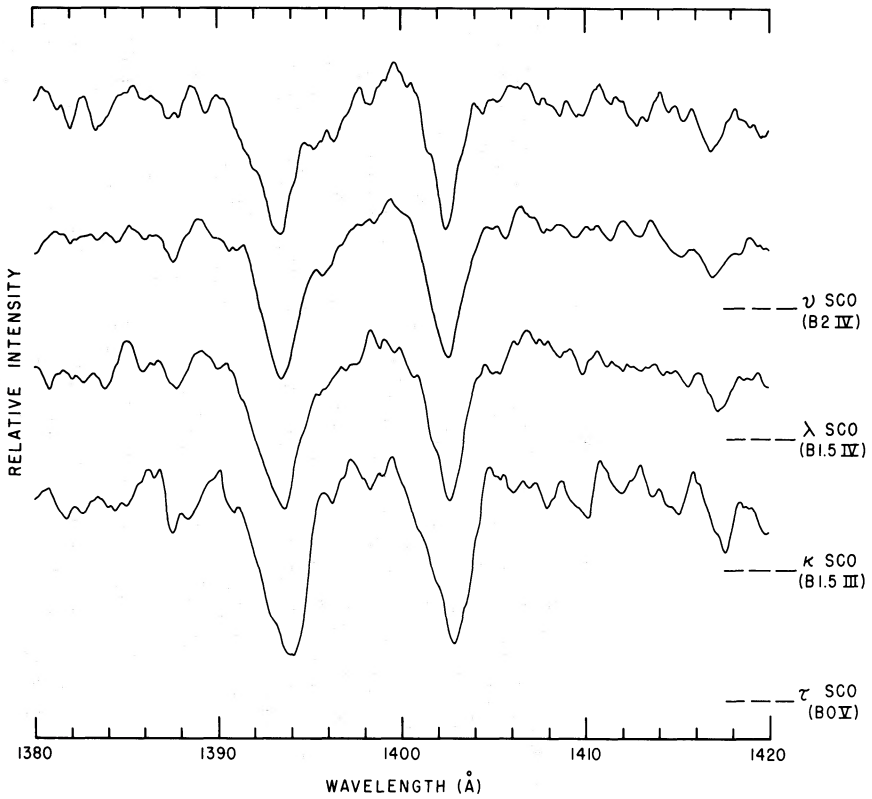

FIG. 4.—Intensity traces of a small region of the high-resolution spectra near the $\lambda\lambda$1393.8, 1402.8 doublet of Si IV. The dashed lines at the right indicate the zero level for each curve.

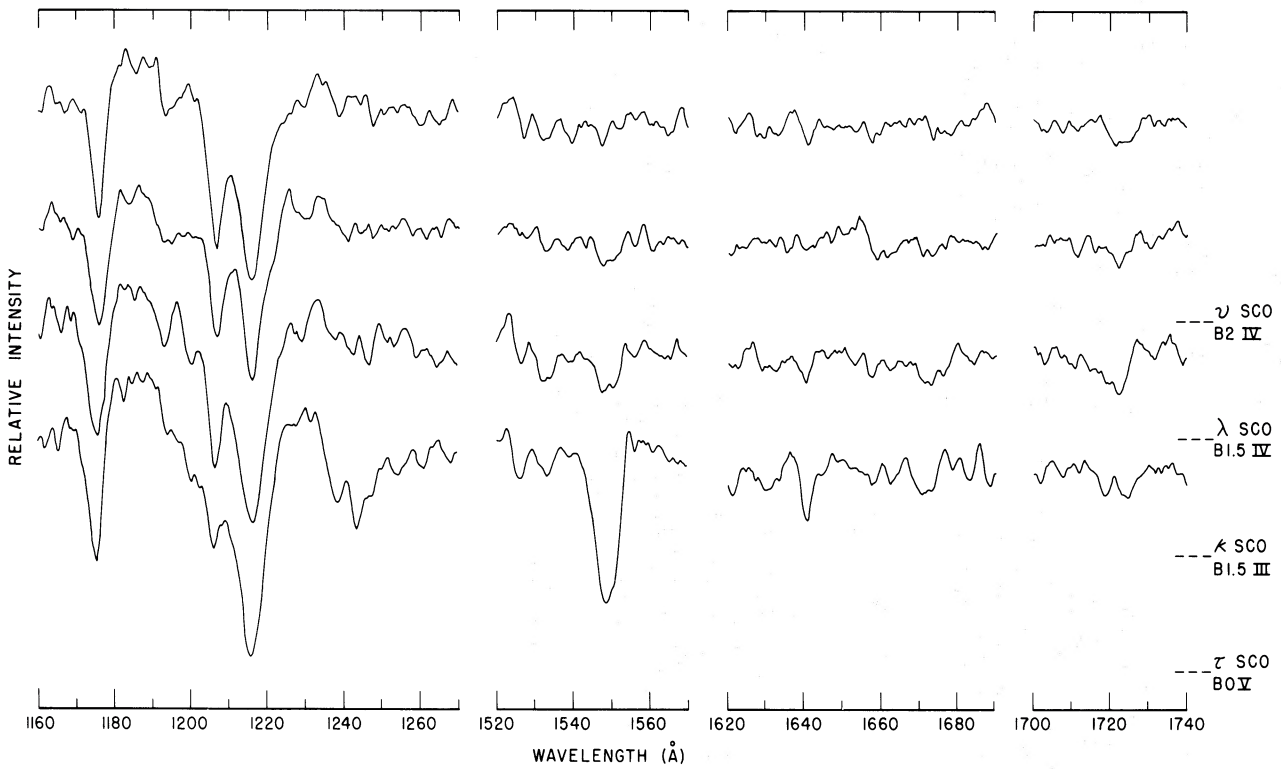

FIG. 5.—Intensity traces of four small regions of the low-resolution spectra. The prominent features are λ1175.7 of C III, λ1206.5 of Si III, λ1215.7 of H I, λλ1238.8, 1240.8 of N V, λλ1548.2, 1550.8 of C IV, λ1640.4 of He II, and a blend near λ1720. The dashed lines at the right indicate the zero level for each curve.

spectra of B stars with low noise and accurate relative intensities. Underhill (1974) has completed an extensive list of line identifications for η CMa (B5 Ia) at 0.2 Å resolution while Rogerson and Upson (1974) are preparing a similar list for τ Sco at 0.05 Å resolution. However, since the *Copernicus* spectra require relatively large and uncertain background corrections between 1450 and 1850 Å, the rocket data are particularly useful in this region. In table 2 we have listed the most reliable lines in the rocket spectra including wavelength regions where there are good *Copernicus* data to provide a basis for checking the reliability of the rocket data. A colon following a wavelength means that the line was clearly distinguishable from the average noise on the intensity trace, but was not easily visible on the photograph. A *b* denotes a relatively broad line, which in many cases may be an unresolved blend. In the high-dispersion spectra, a comparison between laboratory and observed wavelengths of eight lines of Si III, Si IV, O I, and C II gave an rms error of ± 0.15 Å. To allow for possible blends, agreement within ± 0.25 Å was required for identifications. In the low-dispersion regions both of these limits were about a factor 2 larger.

Complete identification of the entries in table 2 will require a detailed analysis of the ultraviolet spectra in conjunction with observations from the ground. Additional far-ultraviolet spectra at a higher dispersion would be useful to resolve blends and extend the wavelength coverage. Meanwhile, the table lists the most probable identifications of the lines along with the multiplet numbers in Moore's (1950–1972) tables. Some additional lines were found in the compilation of Kelly and Palumbo (1973). From 1200 to 1550 Å, there are plausible identifications in the list of Kelly and Palumbo for about 80 percent of the blank spaces in the last column of table 2, but none of them were well enough established to be included here. The spectroscopic tables seemed to be more complete between 1200 and 1400 Å than between 1400 and 1500 Å.

IV. DISCUSSION OF THE SPECTRA

The four stars shown in figures 2 and 3 represent an approximate temperature sequence from 26,200° K (τ Sco) through 21,500° K (λ Sco, κ Sco) to 20,500° K (υ Sco) according to the scale of Morton and Adams (1968), while κ Sco gives some measure of luminosity effects at type B1.5 when compared with λ Sco. Selected portions of the spectra, showing strong lines of C III λ1175.7, Si III λ1206.5, Si IV λλ1393.7, 1402.7, C IV λλ1548.2, 1550.8, and He II λ1640.4 are given in figures 4 and 5. In addition, there is the region near 1720 Å noted as the location of a broad luminosity-dependent feature by Underhill, Leckrone, and West (1972).

As shown in figure 4, the two Si IV resonance lines are present in all four high-dispersion spectra and gradually increase in strength with temperature. This change with temperature is more marked than any

effect of luminosity between κ Sco and λ Sco. The lines are partially resolved even at the lower dispersion, showing that the profiles in τ Sco are asymmetric with additional absorption on the short-wavelength side, indicating outward mass motion. This asymmetry has been confirmed in scans of τ Sco by *Copernicus*. However, as for all the lines shown, the central wavelength is at the stellar wavelength to within ± 0.5 Å, so that the main part of the line is formed in a region of the atmosphere with systematic motions less than 130 km s^{-1}. The edge of the λ1393.7 line in τ Sco corresponds to an outward motion of about 400 km s^{-1}. Morton *et al.* (1972*b*) already have noted evidence for mass motion in the spectrum of ζ Oph (O9.5 V) which is only one spectral subdivision hotter and also on the main sequence. There is a lack of similarity in the two lines of Si IV in υ Sco, suggesting that strong blending is occurring at λ1393 with nearby lines. Hence low-resolution studies of this line might be somewhat compromised if it were to be used as a temperature indicator. On the other hand, λ1402 is relatively free of lines adjacent to it for ± 4 Å from the line center.

On the left of figure 5 the C III λ1175.7 and Si III λ1206.5 lines both show a decrease in central intensity as the temperature increases, though the effect is more marked in Si III than in C III. The ionization potential of C III is 47.9 eV while that for Si III is 33.5 eV, a difference which should significantly influence the relative line strengths. However an important contribution to the λ1206.5 blend is from the ground level of Si III, while the λ1175.7 absorption comes from only an excited level. Nonetheless, in figures 2 and 3 it is evident that the behavior of the Si III multiplet near 1300 Å is quite similar to that of the λ1206.5 feature. Both the C III λ1175.7 and the Si III λ1300 multiplets originate from the ground state of the triplet series, each of which as an excitation of 6.5 eV (± 0.1 eV). According to Osterbrock (1963) the collision strengths and decay rates of these levels are nearly the same. Hence differences in relative ionization, rather than the equilibria of the lower level populations, should explain the differences in the behavior of the C III and Si III features for the temperatures covered here.

The nearness in wavelength of the 1206 and 1175 Å lines may make the ratio Si III/C III a convenient parameter in the classification of ultraviolet spectra from O9 to B5, although the effect of variable interstellar Lα absorption could prove confusing. The changes in Si IV with temperature also are more marked than those of C III, consistent with the strong differences observed for the ionization of Si III already discussed. The behavior of Si III and Si IV qualitatively follows the predictions given by Peytremann (1972).

Figure 5 shows a significant depression in τ Sco that could be due to the N V resonance lines at 1238.8 and 1242.8 Å; but since this exposure occurred at a relatively low altitude, there also could be a contribution from telluric N_2. However, the *Copernicus* spectra confirm that the N V lines are present, so they may provide a useful temperature indicator for the hottest B stars.

The C IV blend ($\lambda\lambda$1548, 1550) shows the most marked change over the small temperature range represented here. The lines provide a good indication of temperature in low-dispersion spectra. For classification purposes, the nearest strong comparison lines which do not change rapidly with temperature would be the Si IV doublet. However, for a uniform set of tracings just the equivalent width of the total C IV feature would be a very sensitive test of temperature. A slight increase in strength may be indicated in going to higher luminosity (λ Sco to κ Sco). The absence of obvious confusing features near the C IV doublet would permit narrow-band photometry to yield an unambiguous index of line strength, though according to Kurucz (1974) the observed C IV lines may involve blends of many weak lines, including particularly Fe III. Considerable experience with UV spectra would be necessary before the contributions of these weak lines could be assessed, though the effect probably is not as critical in classification applications as it is for detailed analyses of the C IV profiles.

The He II 1640 Å line from the 40-eV excited level just becomes apparent in κ Sco. The weakness of this line makes a detailed trend hard to distinguish, although a clear increase occurs between υ Sco and τ Sco.

Underhill *et al.* (1972) have noted an interesting absorption near 1720 Å in supergiants from B0 to A2. They claim that the feature is not observable in main-sequence stars, but at our resolution, better by a factor of 5, all four stars show depressions whose depths exceed 3 σ of the local noise. There appear to be four features represented: one at 1721 Å which increases with temperature, one at 1724 Å which weakens with temperature (B2 to B1.5) and then gives way to a new feature at the same wavelength for B0, and a fourth at 1719 Å which increases with increasing temperature. If these lines are also luminosity-dependent and the absorptions are stronger in supergiants, the temperature effects would explain the presence of the relatively constant depression seen at low resolution over a range in temperatures. The present data are only indicative, and further study of more stars certainly is needed. It is interesting to note that the blend does appear to get stronger between λ Sco and κ Sco.

In summary, the intrinsic strength and large changes of the lines of Si III and C IV may permit a more accurate spectral classification of stars between B0 and B3 than has been demonstrated in this same spectral type region using visible spectra. The Si III and C III lines or the C IV and Si IV lines would be particularly suitable pairs to study owing to their proximity in wavelength. It appears that a resolution of 2 Å is quite sufficient and that even somewhat lower resolution could be useful, in analogy with the 2–4 Å resolution normally used for MK classification. The suggested parameters qualitatively show a greater change between τ Sco and κ Sco than the He I visual line strength between B0 V and B2 V, where these lines are the main temperature indicators for ground-based classification studies (Abt *et al.* 1968; Lesh 1968). Such use of ultraviolet spectra could increase the

precision of spectroscopic parallaxes. With a small satellite such as the *International Ultraviolet Explorer* operating in the low-resolution (6 Å) mode, this work could be extended to the 10th magnitude with little difficulty. For the small sample of stars studied here, however, no strong luminosity indicator has been found, although the 1720 Å region may provide such a parameter when its nature is better understood. One expects that in going to later types, the ratio C II/C III may increase quite sharply, allowing further precision to be obtained in temperature classification from B3 to A0.

The trends noted here with such a small sample of spectra are necessarily suggestive only, since the use of the resonance lines may lead to systematic differences between far-ultraviolet and visual classifications. Understanding these differences, defined by a sufficiently large set of standards, could help considerably in defining a more precise classification system.

The flight of Aerobee KP 3.37 was sponsored by the Kitt Peak National Observatory and was carried out under the direction of R. A. Nidey and R. H. Nagel. M. T. Ruiz assisted in the reduction of the spectra from this flight. This research was supported by contract NSr-31-001-901 from the U.S. National Aeronautics and Space Administration.

REFERENCES

Abt, H. A., Meinel, A. B., Morgan, W. W., and Tapscott, J. W. 1968, *An Atlas of Low-Dispersion Grating Stellar Spectra*.
Jenkins, E. B. 1973, *Ap. J.*, **181**, 761.
Johnson, H. L. 1963, *Basic Astronomical Data*, ed. K. Aa. Strand (Chicago: University of Chicago Press), p. 204.
Kelly, R. L., and Palumbo, L. J. 1973, *Atomic and Ionic Emission Lines Below 2000 Angstroms* (NRL Rept. No. 7599).
Kurucz, R. L. 1974, *Ap. J.* (*Letters*), **188**, L21.
Lesh, J. R. 1968, *Ap. J. Suppl.*, **17**, 371.
Moore, C. E. 1950, 1952, 1962, *NBS Circ.*, No. 488, §§ 1, 2, 3, 4, 5.
———. 1965, 1967, 1970, 1971, 1972, *NSRS-NBS* 3, §§ 1, 2, 3, 4, 6.
Morton, D. C., and Adams, T. F. 1968, *Ap. J.*, **151**, 611.
Morton, D. C., Jenkins, E. B., and Macy, W. W. 1972*a*, *Ap.J.*, **177**, 235.
Morton, D. C., Jenkins, E. B., Matilsky, T. A., and York, D. G. 1972*b*, *Ap. J.*, **177**, 219.
Osterbrock, D. E. 1963, *Planet. and Space Sci.*, **11**, 621.
Peytremann, E. 1972, *Scientific Results from the Orbiting Astronomical Observatory* (*OAO-2*), ed. A. D. Code (NASA SP-310), p. 377.
Rogerson, J. B., Spitzer, L., Drake, J. F., Dressler, K., Jenkins, E. B., Morton, D. C., and York, D. G. 1973, *Ap. J.* (*Letters*), **181**, L97.
Rogerson, J. B., and Upson, W. L. 1974, in preparation.
Uesugi, A., and Fukuda, I. 1970, *Contr. Inst. Ap. and Kwasan Obs., Univ. Kyoto*, No. 189.
Underhill, A. B. 1974, *Ap. J. Suppl.*, **27**, 359.
Underhill, A. B., Leckrone, D. S., and West, D. K. 1972, *Ap. J.*, **171**, 63.

EDWARD B. JENKINS, DONALD C. MORTON, and DONALD G. YORK: Princeton University Observatory, Princeton, NJ 08540

PLATE 1

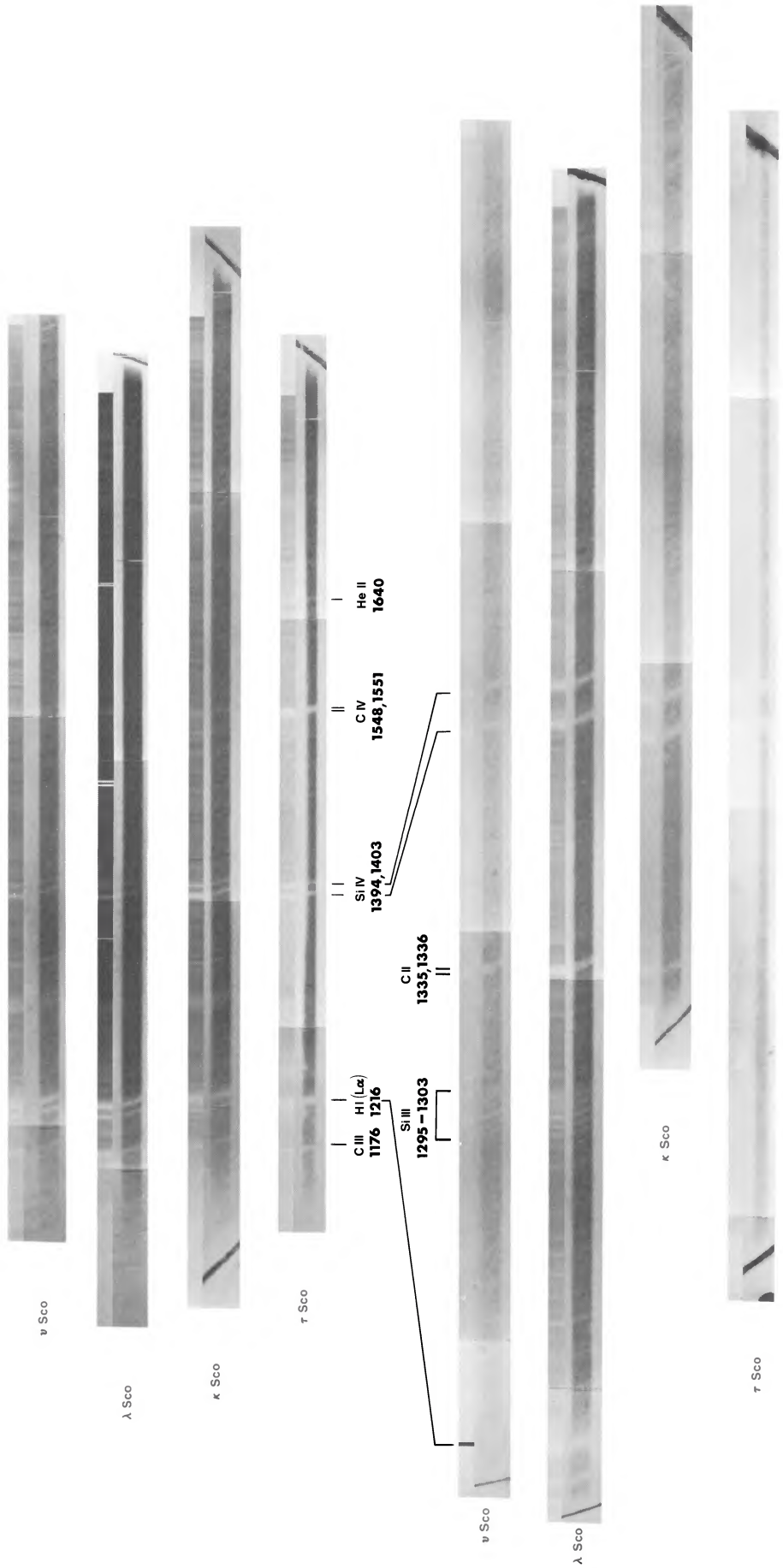

FIG. 1.—Rocket spectra of ν, λ, κ, and τ Sco, with low resolution at the top and high resolution at the bottom. These halftones were reconstructed from digitized two-dimensional densitometer scans of the films. For comparison purposes, above each spectrum in its original form is a band containing vertical striations in density which correspond to the variations in the intensities which were finally derived. The very sharp vertical bars which occasionally appear in either the original spectra or the intensity reconstructions result from digital processing errors and should be disregarded. A zero-order star image is responsible for the feature which looks like an emission line 30 Å longward of the Si IV doublet in the low-resolution spectrum of κ Sco.

JENKINS *et al.* (*see* page 77)